Article

Computational Evidence for Methyl-Donated Hydrogen Bonds and Hydrogen-Bond Networking in 1,2-Ethanediol–Dimethyl Sulfoxide

Robert A. Vergenz, Ibrahim Yazji, Christi Whittington, Jaimee Daw, and King Tu Tran

J. Am. Chem. Soc., **2003**, 125 (40), 12318-12327• DOI: 10.1021/ja036516a • Publication Date (Web): 13 September 2003

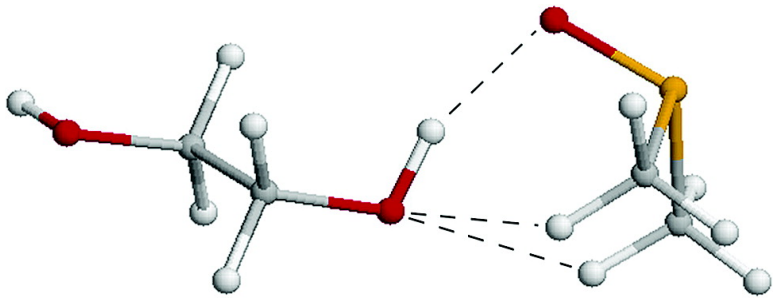

More About This Article

J|A|C|S
ARTICLES
Published on Web 09/13/2003

Computational Evidence for Methyl-Donated Hydrogen Bonds and Hydrogen-Bond Networking in 1,2-Ethanediol−Dimethyl Sulfoxide

Robert A. Vergenz,* Ibrahim Yazji, Christi Whittington, Jaimee Daw, and King Tu Tran

Contribution from the Department of Chemistry and Physics, University of North Florida, Jacksonville, Florida 32224-2645

Received June 5, 2003; E-mail: rvergenz@unf.edu

Abstract: The 1:1 complex of 1,2-ethanediol with dimethyl sulfoxide was studied using density functional theory. A network of three hydrogen bonds holds the complex together, including two in which each methyl group donates to the same hydroxyl oxygen. Four lines of evidence support the existence of methyl-donated hydrogen bonds. The interaction energy is 36 ± 5 kJ/mol using Becke's three parameter hybrid theory with the 1991 nonlocal correlation functional of Perdew and Wang, and a moderately large basis set (B3PW91/6-311++G**//B3PW91/6-31+G**). To determine the energy of each hydrogen bond, a relaxed potential energy scan was performed in a smaller basis set to break the weaker hydrogen bonds by forced systematic rotation of the methyl groups. Two cross-checking analyses show cooperative effects that cause individual hydrogen bond energies in the network to be nonadditive. When one methyl hydrogen bond is broken, the remaining interactions stabilize the complex by storing an additional 2−3 kJ/mol. With all hydrogen bonds intact, the O−H··O−S hydrogen bond contributes 26 ± 2 kJ/mol stability, and each weak methyl bond stores 5 ± 2 kJ/mol.

1. Introduction

Chemistry is the study of the forces that cause atoms or molecules to stick together or break apart. Although more than an order of magnitude weaker than chemical bonds, intermolecular forces play a pivotal role in understanding chemical behavior. Chief among these is hydrogen bonding, with energies up to 170 kJ/mol. They significantly affect the physical properties of specialty materials and solutions, metal hydride and other inorganic complexes, the interactions among organic molecules, and of course, they are crucial to the intricate dance of macromolecules that is biochemistry. The polar and hydrogen-bonding properties of ethylene glycol (EG) are important in its role as a precursor to synthetic nonionic surfactants, as well as in its biochemical activity. Interesting intermolecular interactions result in the appellation of "universal" nonprotic solvent for dimethyl sulfoxide (DMSO).

Participation of methyl groups in donating hydrogen bonds[1] has recently been shown by studies[2] on dimethylformamide to have energy sufficient to contribute to the stability of biological macrostructures. Aromatic CH-donated hydrogen bonds in amino acid residues have been found to be unstable compared to traditional AH··B hydrogen bonds.[3] The strength of the biologically significant NH··O═C hydrogen-bond interaction is classified by Jeffrey[4] as moderate in strength, 17−62 kJ/mol. Recently, networks of hydrogen bonds have been studied in biological systems, such as nucleic acids.[5,6]

Hydrogen bonds are defined by measurable criteria in terms of three concurring properties: (1) hydrogen−acceptor distance in the vicinity of van der Waals overlap, (2) unusual energetic stability, and (3) directional character such that bonding is stronger as the donator−hydrogen−acceptor angle approaches 180°. In traditional hydrogen bonding these three properties function as one definition, because they, in fact, always occur together. A fourth property of some hydrogen bonds is a strong electrostatic character. This seems to be important in systems with nitrogen, oxygen, or fluorine donors, such as in biological systems, but not, for example, in metal hydride hydrogen bonding.

In the Methodology section we present two aspects: information that governed the choice of a basic model chemistry for the study, and important details and assumptions for the methyl rotation relaxed potential energy scan (PES) used to examine the energetics of EG−DMSO. In the first subsection of the Discussion we present four different kinds of evidence leading to the conclusion that there exists a network of hydrogen bonds in the lowest-energy configuration of EG−DMSO that includes two weak interactions that are donated by methyl groups. The

(1) Substituted C−H donation has been known for some time, but not by methyl groups. See: Green, R. D. *Hydrogen Bonding by C−H Groups*; Wiley & Sons: New York, 1974.
(2) Vargas, R.; Garza, J.; Dixon, D. A.; Hay, B. P. *J. Am. Chem. Soc.* **2000**, *122*, 4750−4755.
(3) Scheiner, S.; Kar, T.; Pattanayak, J. *J. Am. Chem. Soc.* **2002**, *124*, 13257−13264.
(4) Jeffrey, G. A. *An Introduction to Hydrogen Bonding*; Oxford University Press: Oxford, 1997; p 12.
(5) Kawahara, S.; Wada, T.; Kawauchi, S.; Sekine, M. *J. Phys. Chem. A* **1999**, *103*, 8516−8523.
(6) Barfield, M.; Dingley, A. J.; Feigon, J.; Grzesiek, S. *J. Am. Chem. Soc.* **2001**, *123*, 4014−4022.

10.1021/ja036516a CCC: $25.00

evidence includes hydrogen−acceptor distances, donor−hydrogen−acceptor angles, electrostatic details of the structure, and indirect geometric indicators of an energy advantage to close methyl contact with an oxygen atom. In the subsequent subsection the structural consequences of breaking the weak methyl hydrogen bonds by methyl rotation are examined. After that two subsections present cross-checking analyses that permit us to assign a distribution of the interaction energy, ΔE, among the three hydrogen bonds. An important caveat to the meaning of hydrogen-bond energies is demonstrated, namely that energy cooperativity occurs within the network when one of the weak interactions is broken. Error sources and limitations of our methodology and conclusions are then discussed. We conclude with some of the implications of the results for research in several areas of chemistry.

2. Methodology

2.1. Choice of Model Chemistry. In applying the quantum theory to the problem of hydrogen bonding, four main procedural issues must be considered: (1) choosing a reliable post-Hartree−Fock method within the constraints of available computational resources, (2) selecting a particular implementation of the method that will produce adequate accuracy, (3) selecting a basis set that does not significantly limit the accuracy of the implementation, and (4) estimating approximate error limits for the results, and their impact on the validity of the conclusions. We address these issues here. Additional attention is given to the fourth issue in subsection 3.5.

Correlation. It is well-known that Hartree−Fock theory alone is intrinsically inadequate for the quantum description of long range interactions. It has been applied with reasonable success in combination with semiempirical strategies to provide potential functions for molecular mechanics in the case of biological macromolecules, where more accurate methods are simply not feasible within the limits of available computers. Fully correlated methods such as configuration interaction and coupled-cluster approaches are highly accurate, but are too computationally intensive for molecules the size of the subject system at most research facilities. Low-order Moller−Plesset perturbation theory (MP2) has been used as a benchmark for calculations on systems the size of EG−DMSO in computational environments where it is feasible. In recent years, density functional theory (DFT) has acquired prominence as an accurate, computationally inexpensive means of accounting for electron correlation.

Density functional theory has recently been an economical method for describing the electronic structure of covalent bonding[7−9] and transition states [10,11] in both organic and inorganic systems. The validity of DFT for hydrogen bonding has been shown through several studies. It has been used successfully for hydrogen bonding in glycine and malonaldehyde,[12] nucleic acid base pairs,[5,6] oxirane−peroxide,[13] and crownophanes.[14] Inorganic hydrogen bonds have also been studied.[15−17]

These successes, in comparison to both MP2 and experiment, may be viewed as unexpected, in that pure DFT has no means by which to adequately describe long-range interactions that are not electrostatic. The DFT models that have been most successful for long-range interactions, though, are the so-called hybrid methods. These are, in essence, semiempirical methods, because the mixing coefficients are derived from performance on a training set of molecules. The validity of the hybrid DFT theories therefore becomes essentially an empirical question, and the spate of successful cases for intermolecular interactions suggests an answer in the affirmative. This is especially understandable in cases with a predominant proportion of electrostatic attraction, as appears to be the case for EG−DMSO.

Implementation and Estimated Error. Our choice of a specific implementation of density functional theory was Becke's three-parameter hybrid functional (B3)[18] with the 1991 nonlocal correlation functional of Perdew and Wang (PW91).[19] This has been demonstrated to be sufficiently accurate for characterizing several hydrogen-bonding systems. Ishida[9] compared B3PW91 and B3 with the correlation functional of Lee, Yang, and Parr (B3LYP) to MP2 results for protonation of a series of alkylamines. The MP2 results were in the range from 0.7 to 2.5 kJ/mol. They found that interaction energies by both DFT methods are within 1−2 kJ/mol of the MP2 results. Sirois compared different DFT models to MP2 energies of 12 organic hydrogen-bond energies that range from 2 to 45 kJ/mol. He concluded that B3PW91, B3LYP, and two different Laplacian functionals all produced results within 1−3 kJ/mol of the MP2 results.[12]

Only for inorganic hydrogen bonding do the hybrid methods give mixed results. Orlova, et. al.[15,16] studied the hydrogen bonding of the inorganic hydride complex $Mo(CO)_2(PH_3)_2(NO)H\cdot\cdot HF$, comparing B3LYP, BLYP, and B3PW91 to the experimental ΔE of 28 kJ/mol. All the DFT theories overestimated this energy, B3PW91 by 14−16 kJ/mol, the other two by 20−24 kJ/mol. Clot, et. al. calculated hydrogen-exchange energies for an iridium−ammonia−HF complex using B3PW91 and compared the difference of rotated amine groups to a variable-temperature NMR free energy change of 49.6 kJ/mol and found agreement within about 0.8 kJ/mol.[17] Inconsistent performance for these systems makes sense because these hydrogen bonds often have only slight electrostatic components.

Our choice of B3PW91 is based on the similarities between our system and other hydrogen-bonding networks successfully studied using B3PW91.[5,6,12] These studies show that B3PW91 provides an adequate compromise between computational cost and accuracy in such systems. Comparing accuracies from these studies on organic hydrogen-bonding systems, in which the nature of the interactions are similar to our system, we estimate that B3PW91 can provide interaction energies for EG−DMSO that are probably accurate to about 4 kJ/mol.

The Gaussian-98W software package[20] was used on several different Pentium-II, -III, and -IV desktop computers. All calculations include all core and valence electrons in calculating energy expectation values. All ΔE in this study were calculated using the counterpoise method. Electrical charge was distributed to the atoms in the EG−DMSO complex with Mulliken population analysis. Although Mulliken analysis is only one of several possible ways to assign charges to the nuclei, it is a reasonable and conceptually simple means to examine electrostatic charges for our purposes.

Basis Set. To select an appropriate basis set, quantum structure calculations using B3PW91 with various basis sets were performed on

(7) Fangstrom, T.; Edvardsson, D.; Ericsson, M.; Lunell, S.; Enkvist, C. *Int. J. Quantum Chem.* **1998**, *66*, 203−217.
(8) Braïda, B.; Hiberty, P. C. *J. Phys. Chem. A* **1998**, *102*, 7872−7877.
(9) Ishida, H. *Z. Naturforsch.* **2000**, *55a*, 769−771.
(10) Durant, J. L. *Computational Thermochemistry*; American Chemical Society: Washington, DC, 1998; Chapter 14. See also Durant, J. L. *Chem. Phys. Lett.* **1996**, *256*, 595−602.
(11) Cui, Q.; Liu, Z.; Morokuma, K. *J. Chem. Phys.* **1998**, *109*, 56−62.
(12) Sirois, S.; Proynov, E. I.; Nguyen, D. T.; Salahub, D. R. *J. Chem. Phys.* **1997**, *107*, 6770−6781.
(13) Portmann, Stefan.; Inauen, A.; Luethi, H. P., Leutwyler, S. *J. Chem. Phys.* **2000**, *113*, 9577−9585.
(14) Tsuzuki, S.; Luthi, H. P. *J. Chem. Phys.* **2001**, *123*, 4255−4258.
(15) Orlova, G.; Scheiner, S. *J. Phys. Chem. A* **1998**, *102*, 260−269.
(16) Orlova, G.; Scheiner, S. *J. Phys. Chem. A* **1998**, *102*, 4813−4818.
(17) Clot, E.; Eisenstein, O.; Crabtree, R. H. *New J. Chem.* **2001**, *25*, 67−72.
(18) Becke, A. D. *J. Chem. Phys.* **1996**, *104*, 1040.
(19) Perdew, J. P.; Burke, K.; Wang, Y. *Phys. Rev. B* **1996**, *54*, 1653.
(20) Frisch, M. J.; Trucks, G. W.; Schlegel, H. B.; Scuseria, G. E.; Robb, M. A.; Cheeseman, J. R.; Zakrzewski, V. G.; Montgomery, J. A., Jr.; Stratmann, R. E.; Burant, J. C.; Dapprich, S.; Millam, J. M.; Daniels, A. D.; Kudin, K. N.; Strain, M. C.; Farkas, O.; Tomasi, J.; Barone, V.; Cossi, M.; Cammi, R.; Mennucci, B.; Pomelli, C.; Adamo, C.; Clifford, S.; Ochterski, J.; Petersson, G. A.; Ayala, P. Y.; Cui, Q.; Morokuma, K.; Malick, D. K.; Rabuck, A. D.; Raghavachari, K.; Foresman, J. B.; Cioslowski, J.; Ortiz, J. V.; Stefanov, B. B.; Liu, G.; Liashenko, A.; Piskorz, P.; Komaromi, I.; Gomperts, R.; Martin, R. L.; Fox, D. J.; Keith, T.; Al-Laham, M. A.; Peng, C. Y.; Nanayakkara, A.; Gonzalez, C.; Challacombe, M.; Gill, P. M. W.; Johnson, B. G.; Chen, W.; Wong, M. W.; Andres, J. L.; Head-Gordon, M.; Replogle, E. S.; Pople, J. A. *Gaussian 98*, revision 5.2; Gaussian, Inc.: Pittsburgh, PA, 1998.

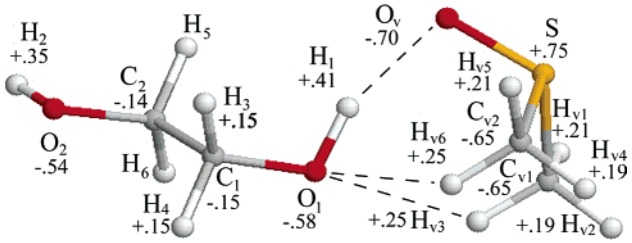

Figure 1. Lowest-energy interaction of 1,2-ethanediol with dimethyl sulfoxide in B3PW91/6-311++G**//B3PW91/6-31+G** model chemistry, with atomic electrostatic charges from Mulliken population analysis of the electron density.

Table 1. Basis Set Dependence of Interaction Energy (kJ/mol) of Ethylene Glycol−Dimethyl Sulfoxide by Counterpoise Method with Density Functional Theory

		diffuse functions		
basis set	polarization	none	+	++
6-31G	none	48.2	47.0	46.8
	*	35.9	35.1	35.0
	**	36.1	35.9	35.8
6-311G	none	47.8	47.6	47.5
	*	37.0	37.2	37.1
	**	35.9	36.3	36.2

a 1:1 complex of EG and DMSO. Table 1 explores the dependence of the interaction energies on basis set. Diffuse functions affect energies by only 0.1−0.5 kJ/mol. Polarization, however, is seen to be important to adequately describe the interaction. The final reported ΔE of 36 kJ/mol for EG−DMSO is in the B3PW91/6-311++G**//B3PW91/6-31+G** model chemistry. The lowest-energy structure is shown in Figure 1. An estimate of the accuracy of this model chemistry, including both method and basis set errors, would thus be about 5 kJ/mol.

2.2. Relaxed Methyl Rotation Potential Energy Scan. To examine the energy needed to break a weak hydrogen bond, a relaxed potential energy scan (PES) was performed. The lowest-energy geometry of Figure 1 was altered by a systematic rotation of the methyl groups, with all other nuclear coordinates relaxed to a minimum of energy consistent with this constraint. The PES was done over the entire 120° rotation range of the C_{3v} symmetry group for both methyl groups in the B3PW91/6-31G* model, using 10° steps. The counterpoise method was used to calculate interaction energies throughout the grid. In this work, atoms are numbered conventionally, except that DMSO is arbitrarily denoted as solvent and "v" is added to its atom subscripts where confusion would otherwise occur.

The dihedral angles $D(O_v-S-C_{v1}-H_{v1})$ and $D(O_v-S-C_{v2}-H_{v4})$ describe the rotation relative to O_v of methyl-1 and methyl-2, respectively, and each point in the scan is represented by an ordered pair, $(D(O_v-S-C_{v1}-H_{v1}), D(O_v-S-C_{v2}-H_{v4}))$, rounded to the nearest whole degree for reference only. The lowest-energy configuration is thus denoted (68°, 174°), and the upper-left and lower-right corners of the surrounding grid are designated (8°, 104°) and (128°, 224°), respectively.

Convergence of the constrained geometry optimizations was very slow because this weakly bound system is "floppy," that is, substantial changes in several of the internal coordinates leads to insignificant change in energy. Gaussian-98W normally uses four criteria to judge the convergence of a geometry optimization: average and maximum coordinate displacement, and average and maximum energy derivative with respect to coordinates. In cases where the energy derivatives are less than one-tenth of the convergence criteria, that is, for "floppy" molecules, the displacement criteria are disregarded. Despite this provision, several of the conformations around the periphery of the PES grid required in excess of 100 iterations to converge.

Achieving convergence was further complicated for several of the PES grid points by the existence of one or more constrained local minima with energies only slightly above the constrained absolute minimum. The constrained absolute and local minimum energy conformations are similar in appearance to those shown in Figure 2, a, b, and c, which illustrate conformations with weak methyl hydrogen bonds involving only methyl-1, only methyl-2 and both methyl groups, respectively. Which of these types of conformations is lowest in energy changes from one region of the PES grid to another. Typically, in the center and upper right regions of the PES grid the lowest-energy conformation is similar to Figures 1 and 2c, to the left of center the conformation tends to be like Figure 2a, and to the lower right of center like Figure 2b. Whether convergence of the calculation is to an absolute or local minimum depends on the initial input conformation. In one case, (128°, 204°), convergence was not achieved despite a variety of standard remedies, because the optimization algorithm oscillated between the minima. This data point was not used in drawing conclusions.

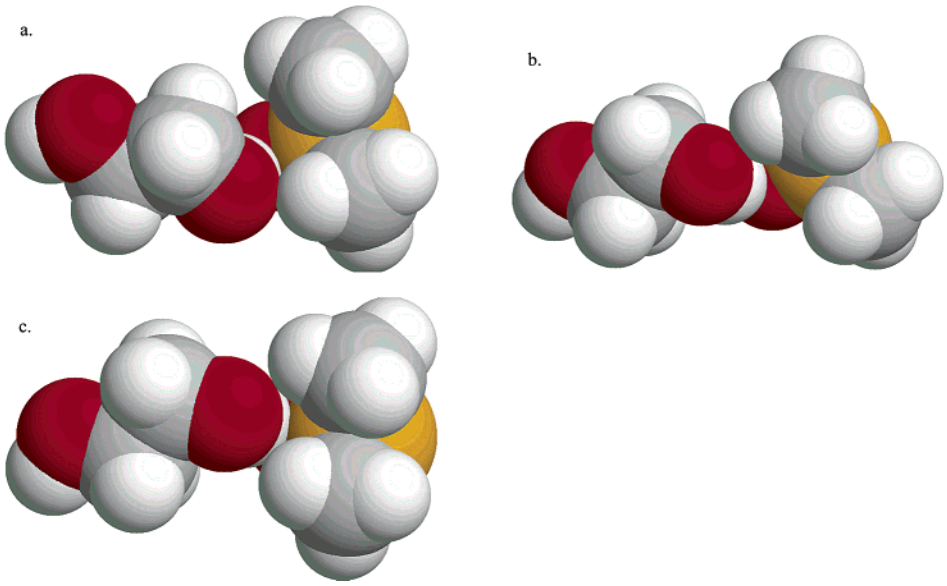

Figure 2. Space-filling rendition of representative conformations from relaxed potential energy scan of methyl rotations in 1,2-ethandiol with dimethyl sulfoxide in B3PW91/6-31G*, with $(D(O_v-S-C_{v1}-H_{v1}), D(O_v-S-C_{v2}-H_{v4}))$ given. (a) Methyl-1 only weak hydrogen bond, (78°, 224°), (b) Methyl-2 only weak hydrogen bond, (68°, 114°), and (c) Transition structure with both methyl groups hydrogen bonded, (68°, 134°).

Table 2. Geometric Description of Hydrogen Bonding of 1,2-Ethanediol/Dimethyl Sulfoxide in B3PW91/6-31+G** Model Chemistry

AH··B	RHB (Å)	RAB (Å)	∠(AHB) (deg)	RAH (Å)
$O_1-H_1\cdot\cdot Ov$	1.79	2.74	159.7	0.98
$C_{v1}-H_{v3}\cdot\cdot O_1$	2.54	3.36	130.7	1.09
$C_{v2}-H_{v6}\cdot\cdot O_1$	2.61	3.41	129.9	1.09
moderate H bond[a]	1.5−2.2	2.5−3.2	130−180	- -
weak H bond[a]	2.2−3.2	3.2−4.0	90−150	- -

[a] See ref 4.

Because we wish to examine the energies of both weak methyl hydrogen bonds, all three of these minima are of interest. Because they are sometimes within about 1 kJ/mol of each other, they are roughly equally accessible at room temperature. Therefore, we decided to force inclusion of all three in the PES grid, even though they may represent a local and not an absolute energy minimum in some cases. For example, consider the constraint-optimized conformations corresponding to methyl rotation angles of (128°, 224°), (128°, 104°), and (8°, 224°), with relative energies 27.5, 28.1 and 28.5 kJ/mol, respectively. In these conformations the methyl-1 rotation angles differ from each other by exactly120°, and likewise for the methyl-2 angles. Thus, with the methyl C_{3v} symmetry, the six methyl hydrogen atoms in all three conformations are identical in location, and merely differ in label assignments, and therefore also in the order in which they are considered in the geometry optimization algorithm. The first of these points corresponds to a constrained absolute minimum with structure similar to that in Figure 2a, while the latter two are constrained local minima corresponding to structures as in Figure 2, b and c, respectively. By our choice of initial input conformation, we indirectly required that points with methyl-2 angles less than 174° (the value for the absolute lowest-energy configuration) converge to structures such as Figure 2, b or c, while those with methyl-2 angles higher than 174° converged to structures such as those in Figure 2, a or c. This ensured that we could examine the breakage of both methyl hydrogen bonds, although more points were obtained which broke the methyl-1 bond than which broke the methyl-2 bond. For eight of the grid points, careful choice of initial geometry was necessary for convergence to the desired minimum energy conformation.

3. Results and Discussion

3.1. Evidence of Methyl-Donated Hydrogen Bonds in EG−DMSO. Figure 1 shows the lowest-energy configuration of EG−DMSO in the B3PW91/6-311++G**//B3PW91/6-31+G** model chemistry. Note the well-known hydrogen bonding between H_1 and O_v, and the nearly linear hydrogen bond angle, $A(O_1-H_1-O_v)$. The dihedral angle $D(H_1-O_1-C_1-C_2)$ is 72.7°. This gauche effect[21] is not uncommon but deviates significantly from the commonly expected value of 180° and also from $D(H_2-O_2-C_2-C_1)$, which is 178.6°. The space-filled representation of Figure 2 makes clear the near or complete van der Waals contact between one hydrogen atom from the methyl groups and the hydroxyl oxygen. The lowest-energy configuration is similar in methyl−oxygen approach distances to those shown in Figure 2c.

Table 2 presents internuclear distances and angles in the optimized structure that are relevant to possible hydrogen bonding. Also included is structure information used by Jeffrey[4] to categorize hydrogen bonds as strong, moderate, and weak. Judging by the criteria of internuclear distances and angles, we conclude that H_1-O_v is a moderate hydrogen bond and that $H_{v3}-O_1$ and $H_{v6}-O_1$ have properties consistent with weak to moderate hydrogen bonds.

Although not definitive, electrostatic information can be helpful in recognizing hydrogen bonds. Included in Figure 1 is the distribution among the nuclei of electrical charge in atomic units (au), as determined by Mulliken population analysis. The charge distribution makes clear that electrostatic considerations favor formation of methyl hydrogen bonds in this complex. The sulfonyl dative bond is strongly polarized, as expected, but the $S-C_v$ bonds are almost as strongly polarized. This induces sufficient polarity in the methyl C−H bonds to act as hydrogen bond donors. The largest and smallest methyl C−H charge differences are 0.90 and 0.84 au, respectively. This compares well with the charge differences along the O−H bonds in EG of 0.99 and 0.89 au, but is in contrast to the relatively nonpolarized methylene C−H bonds of EG, with a charge difference of only 0.30 au. Despite the low electronegativity of carbon, the methyl$-O_1$ interactions seem to have significant electrostatic stabilization.

The binding energy of 36 kJ/mol for the EG−DMSO complex is certainly consistent with hydrogen bonding, but this could conceivably be attributed entirely to the traditional hydroxyl-donated hydrogen bond. There is, however, evidence in the geometric details of the lowest-energy configuration which indirectly shows there is an energetic advantage to methyl-donated hydrogen bonds in EG−DMSO. The methyl groups are rotated an average of 9° inward from the ideal staggering of 60° from O_v, with $D(O_v-S-C_{v1}-H_{v3})$ and $D(O_v-S-C_{v2}-H_{v6})$ of 51.3° and 51.7°, respectively. This moves H_{v3} and H_{v6} closer to O_1, and opens the angles $A(C_{v1}-H_{v3}-O_1)$ and $A(C_{v2}-H_{v6}-O_1)$ a few degrees closer to linearity. It happens despite the resulting increased repulsive interaction between the two methyl groups. These structural features demonstrate that there is a compensating energetic advantage to the close contact of both methyl hydrogen atoms with O_1 and that these contacts are not merely forced repulsive interactions of the type described by Jeffrey.[4] We have thus established the existence of weak methyl-donated hydrogen bonds in EG−DMSO on the basis of four criteria: (1) interaction distances, (2) angles consistent with hydrogen bonding, (3) the electrostatic character of the methyl C−H bonds, and (4) indirect geometric evidence of an energetic advantage in the close methyl-O_1 contacts.

3.2. Effect of Methyl Rotations on Methyl-Donated Hydrogen Bonds. The energy criterion for hydrogen bonding is perhaps physically and historically the most important. Yet, it is intrinsically ambiguous in the case of a network of hydrogen bonds, unless each hydrogen bond in the network can be assigned a specific portion of the total binding energy. Since hydrogen bonds, more so than covalent bonds, have energies that vary widely from one complex to another, and are strongly dependent on distance and angle, it is possible that the energy of a hydrogen bond within a network might not be constant, but may vary with parameters that affect distance and angle.

We desire to understand the effect on the energy of breaking the methyl$-O_1$ interactions. To accomplish this, we performed a relaxed PES, as described in subsection 2.2. The movement of methyl hydrogen atoms in many cases resulted in breaking their close contact with O_1. Figure 3 shows the resulting total energies. Cross-sections of this three-dimensional plot passing through the lowest-energy configuration in the direction of

(21) Goodman, L. Private communication, poster at *Sanibel Symposium*, St. Augustine, FL, 2003.

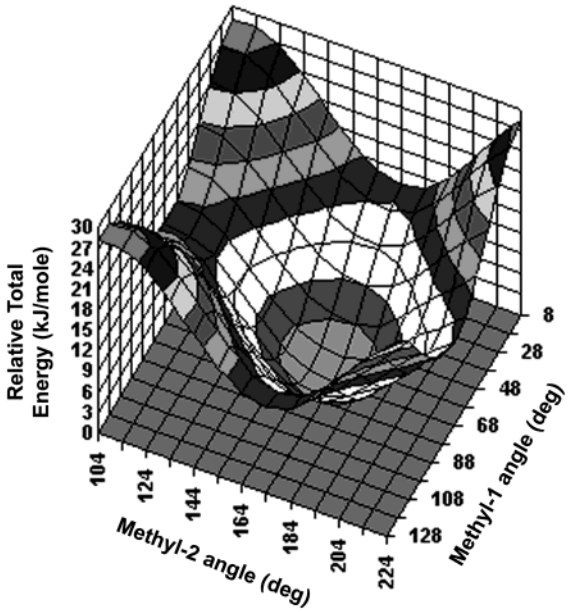

Figure 3. Total energy as a function of rotation of methyl groups in relaxed potential energy scan of 1,2-ethanediol−dimethyl sulfoxide in B3PW91/6-31G* model chemistry. Contour interval is 3 kJ/mol.

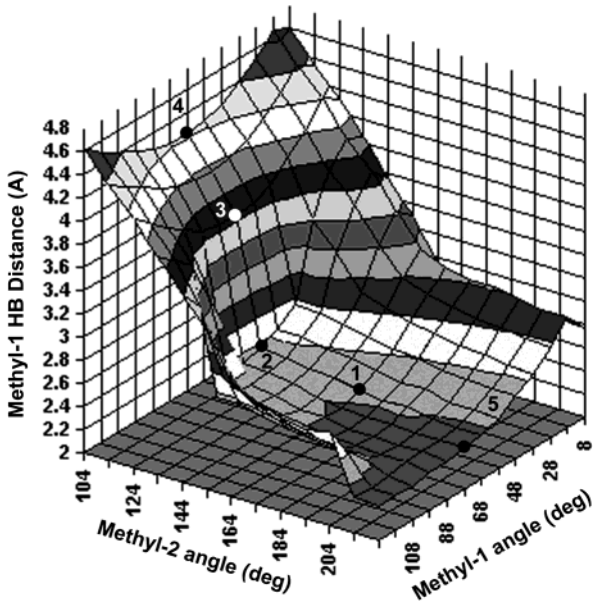

Figure 4. Methyl-1 weak hydrogen bond distance, R_1, as a function of rotation of methyl groups in relaxed potential energy scan for 1,2-ethanediol−dimethyl sulfoxide. Contour interval is 0.2 Å. Labeled conformations are: 1 = (68°, 174°), lowest-energy; 2 = (68°, 134°), transitional; 3 = (68°, 124°), cooperative methyl-2 H bonded; 4 = (68°, 104°), extreme methyl-2 H bonded; 5 = (78°, 224°), methyl-1 H bonded.

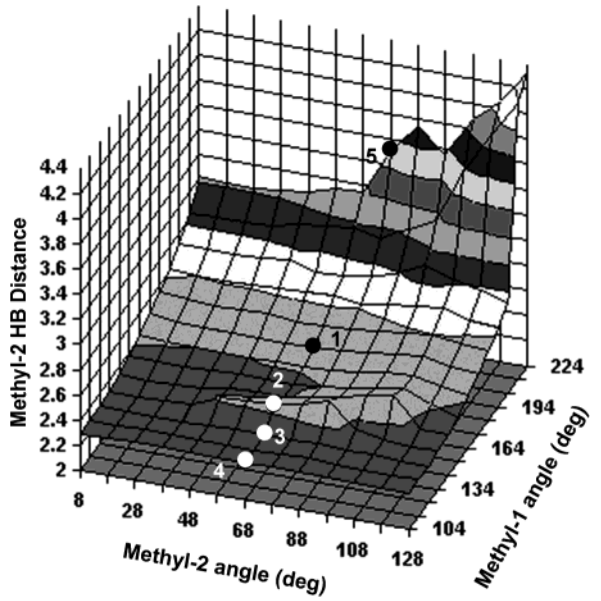

Figure 5. Methyl-2 weak hydrogen bond distance, R_2, as a function of rotation of methyl groups in relaxed potential energy scan for 1,2-ethanediol−dimethyl sulfoxide. Contour interval is 0.2 Å. Labeled conformations are: 1 = (68°, 174°), lowest-energy; 2 = (68°, 134°), transitional; 3 = (68°, 124°), cooperative methyl-2 H bonded; 4 = (68°, 104°), extreme methyl-2 H bonded; 5 = (78°, 224°), methyl-1 H bonded.

constant methyl-1 angle or of constant methyl-2 angle, show the classic shape of a methyl rotation barrier. This indicates that any effect of the methyl hydrogen bonding on the energy is small in comparison to the rotation barrier.

We examine the effectiveness of the methyl rotations at breaking the weak hydrogen bonds by noting the effects on the methyl−oxygen distance. Define the distance between acceptor and hydrogen atoms in each hydrogen bond as R_i, with $i = 0$, 1, and 2 referring to the moderately strong hydrogen bond, the methyl-1 hydrogen bond, and the methyl-2 hydrogen bond, respectively. We found R_0 to be constant over the entire PES grid at 1.79 ± 0.01 Å. Figure 4 displays R_1 for the entire methyl rotation PES grid, and Figure 5 gives this information for R_2. The most prominent features in Figures 4 and 5 are abrupt transitions from short R_i to longer R_i with only slight changes in the methyl rotation angles. In Figure 4, starting from the lowest-energy configuration at (68°, 174°), labeled 1, and reducing the methyl-2 angle by 40°, to the conformation labeled 2, changes R_1 only slightly. Rotating methyl-2 by only an additional 10°, to (68°, 124°), labeled 3, increases R_1 by more than 1 Å, corresponding to the breaking of the methyl-1 weak hydrogen bond. Figure 5 shows a similar behavior of R_2 in the lower-right region of the PES grid, although it extends over a smaller part of the methyl rotation space. Clearly, methyl rotations had the intended effect of breaking the weak methyl hydrogen bonds in some of the conformations.

It is informative to examine the structure of the conformations represented in Figures 3, 4, and 5. They fall into three main types, with some transitional structures between the types. Representative examples of each type are shown in Figure 2, a, b, and c, corresponding to the grid points (78°, 224°), (68°, 114°), and (68°, 134°). These conformations are labeled 5, 3, and 2, respectively, in Figures 4−8, and illustrate structures with weak methyl hydrogen bonds involving only methyl-1, only methyl-2, and both methyl groups, respectively. We observe that when methyl rotations put sufficient strain on the weak methyl hydrogen bonds and the complex is allowed to relax, the intermolecular coordinates shift so that one of the methyl groups swings away from contact with O_1. Therefore, nearly degenerate conformations such as Figure 2, a and b, are possible at most points on the PES grid.

To understand the details of the structural transition from two methyl hydrogen bonds to only one, Table 3 lists the values for those independent internal coordinates that are principally responsible for the structural change. Bond angles that change less than 1° and dihedral angles that change less than 2° from the lowest-energy configuration are omitted. Dihedral angle

Table 3. Internal Coordinates Relevant to Structural Transitions among Selected Methyl Rotation PES Conformations of Ethylene Glycol−Dimethyl Sulfoxide

R=distance (Å), A=bond angle (deg), D=dihedral angle (deg)	two methyl H bonds		one methyl H bond on methyl-2		5. one methyl H bond on methyl-1[a]
	1. lowest *E* (68,174)[a]	2. transitional (68,134)[a]	3. cooperative (68,124)[a]	4. extreme (68,104)[a]	(78,224)
$R(H_1,O_v)$	1.80	1.78	1.78	1.79	1.79
$R(H_{v3},O_1)$	2.45	2.56	3.64	4.22	2.35
$R(H_{v6},O_1)$	2.45	2.44	2.30	2.30	3.52
$A(C_1,O_1,H_1)$	109.1	109.1	107.7	107.5	108.4
$A(O_1,H_1,O_v)$	158.8	159.3	163.7	163.2	161.9
$A(C_{v1},H_{v3},O_1)$	131.3	130.2	–	–	136.8
$A(C_{v2},H_{v6},O_1)$	131.8	129.6	145.6	143.7	–
$A(H_1,O_v,S)$	107.2	108.5	116.2	117.6	111.1
$A(O_v,S,C_{v1})$	106.9	105.7	106.1	106.6	107.8
$A(O_v,S,C_{v2})$	106.8	107.4	107.8	108.1	107.0
$A(H_{v1},C_{v1},H_{v3})$	109.9	110.2	110.0	109.8	111.0
$A(S,C_{v2},H_{v4})$	109.8	110.9	111.3	111.8	109.1
$A(S,C_{v2},H_{v5})$	106.9	109.3	109.1	108.7	105.0
$A(S,C_{v2},H_{v6})$	108.5	106.0	105.9	106.0	112.6
$D(C_2,C_1,O_1,H_1)$	72.6	72.1	75.3	74.2	75.8
$D(C_1,O_1,H_1,O_v)$	155.3	168.4	104.5	92.4	115.1
$D(O_1,H_1,O_v,S)$	0.9	5.9	33.4	34.0	2.6
$D(H_1,O_v,S,C_{v2})$	−51.8	−47.6	−23.0	−2.8	−66.5
$D(O_v,S,C_{v1},H_{v1})$[b]	67.8	67.8	67.8	67.8	77.8
$D(O_v,S,C_{v2},H_{v4})$[b]	173.9	133.9	123.9	103.9	223.9
$D(O_v,S,C_{v2},H_{v5})$[b]	−67.3	−103.1	−113.6	−134.3	−19.8
$D(O_v,S,C_{v2},H_{v6})$[b]	51.4	16.7	5.8	−15.3	99.4

[a] Sequential integers identify conformations explicitly labeled in Figures 4−8. [b] Internal coordinates artificially manipulated, or those directly dependent on artificial manipulation.

changes that were imposed artificially in the PES, and those directly dependent on the artificial changes, are noted with an asterisk. No covalent bond distances in these conformations vary from the lowest-energy configuration by more than 0.02 Å. In the first two columns are coordinates for the lowest-energy configuration of the complex, (68°, 174°), and for (68°, 134°), which closely resembles it despite the transition over a 40° rotation of methyl-2. These are pictured in Figures 1 and 2c, respectively, and labeled 1 and 2, respectively, in Figures 4−8. The most significant changes between these conformations are in three of the intermolecular dihedral angles: $D(C_1,O_1,H_1,O_v)$ increases by 13°, and $D(O_1,H_1,O_v,S)$ and $D(H_1,O_v,S,C_{v2})$ each increase by 4−5°. Also noteworthy is that the methyl-2 bond angles are distorted 2−3° to help maintain contact of H_{v6} with O_1. The methyl distortion is also manifested in that changes in the methyl dihedral angles for H_{v5} and H_{v6} are a few degrees different than the 40° change imposed on H_{v4} of the same methyl group.

The next column of Table 3, labeled "cooperative" for reasons that will be made clear later, quantifies the dramatic structural changes that result from an additional 10° rotation of methyl-2. This conformation corresponds with Figure 2b, and is labeled 3 in Figure 4. The intermolecular dihedral angles $D(C_1,O_1,H_1,O_v)$, $D(O_1,H_1,O_v,S)$, and $D(H_1,O_v,S,C_{v2})$ are now different by −51°, 33° and 29°, respectively, from the lowest-energy configuration. This accomplishes the swinging away of methyl-1 from contact with O_1. The reason this happens is clear from the increases of 5° and 9°, respectively, in the moderate hydrogen bond angle $A(O_1,H_1,O_v)$ and the supporting intermolecular angle $A(H_1,O_v,S)$. One expects the opening up of the hydrogen bond angle to strengthen the stability of that interaction, as is quantitatively confirmed in the next two subsections. Distortion of the methyl-2 angles is also partially alleviated by these conformational changes. The network of three hydrogen bonds, one moderate and two weak, thus creates an environment where cooperative effects are possible: breaking one of the weak hydrogen bonds enables geometry adjustments that serve to strengthen the other intermolecular interactions. The column of Table 3 with extreme rotation of methyl-2 to the (68°, 104°) conformation is discussed along with topics in subsection 3.4.

The last column of Table 3 shows the corresponding changes in the (78°, 224°) conformation, representative of those in which methyl-2 swings away from contact with O_1, and the methyl-1 hydrogen bond remains. This corresponds to the structure in Figure 2a. The same qualitative changes occur as in the (68°, 124°) conformation, though they are of lesser magnitude because of the different methyl rotation angles. Also contributing to energy differences between structures in Figure 2, a and b, is the symmetry breaking caused by the gauche effect on the O_1-H_1 bond, as described in subsection 3.1.

3.3. Energies of the Hydrogen Bond Network: Two-Point Method. We quantified hydrogen bond energies and cooperativity effects by two methods. The first method we call the two-point method, because we consider only a pair of conformations out of the 169 methyl rotation PES grid points. It is similar to methods used in previous work.[12,15,17] Conformation A has all three hydrogen bonds intact, while B has only two, one moderate and one weak. Conformation B results from A after a 50°−60° rotation of one of the methyl groups, to break one of the weak methyl hydrogen bonds and induce the conformational changes described above. The interaction energy of each conformation, designated ΔE_A and ΔE_B, respectively, is calculated by the counterpoise method. We also calculate the counterpoise interaction energies of additional conformations C and D, which result from conformations A and B, respectively, by rotating the entire DMSO molecule 180° about the $S-O_v$ axis without permitting any subsequent relaxation of the complex. This latter rotation removes both methyl groups from contact with O_1, while presumably leaving the moderate hydrogen bond unaltered. Because we did not allow conformations C and D to relax, all intramolecular coordinates of both

Table 4. Results of the Two-Point Method for Distributing EG−DMSO Interaction Energy among Moderate and Weak Hydrogen Bonds and Cooperativity

conformation with three H bonds	conformation with two H bonds	E_{mod} (kJ/mol)	E_{weak} (kJ/mol)	ΔE_{mod} (kJ/mol)	ΔE_{weak} (kJ/mol)	E_{coop} (kJ/mol)
(78,174)	(78,114)	26.0	5.0	0.9	0.9	1.9
(68,174)	(68,124)	26.3	4.8	0.7	1.9	2.6
(58,174)	(58, 114)	26.2	4.7	0.4	2.0	2.4
	average ± SD	26.2 ± 0.2	4.8 ± 0.2			2.3 ± 0.4

EG and DMSO are unchanged from conformation A or B, respectively.

We can then assign physical significance to the binding energies, designating the moderate strength of the $H_1 \cdot\cdot O_v$ bond as E_{mod}, and that of a single methyl hydrogen bond as E_{weak}. We designate any cooperative effects, in which energy is shifted on breaking a hydrogen bond, as $E_{coop} = E_{coop,mod} + E_{coop,weak}$, where the right-hand side indicates the intermolecular interactions which putatively store energy. With these definitions we can assign on physical grounds that

$$\Delta E_A = E_{mod} + 2\,E_{weak} \tag{1a}$$

$$\Delta E_B = E_{mod} + E_{weak} + E_{coop,mod} + E_{coop,weak} \tag{1b}$$

$$\Delta E_C = E_{mod} \tag{1c}$$

$$\Delta E_D = E_{mod} + E_{coop,mod} \tag{1d}$$

Inclusion of E_{coop} terms in eqs 1 does not presuppose the existence of cooperative effects, since the equations do not preclude the possibility that $E_{coop} = 0$. Given the calculated interaction energies, eqs 1 can be solved for the unknowns to give

$$E_{mod} = \Delta E_C \tag{2a}$$

$$E_{weak} = (\Delta E_A - \Delta E_C)/2 \tag{2b}$$

$$E_{coop} = \Delta E_B - (\Delta E_A + \Delta E_C)/2 \tag{2c}$$

with $E_{coop,mod} = \Delta E_D - \Delta E_C$ and $E_{coop,weak} = \Delta E_B - \Delta E_D - (\Delta E_A - \Delta E_C)/2$. In principle the equations for $E_{coop,mod}$ and $E_{coop,weak}$ are valid if there are no other contributing intermolecular interactions, such as hyperconjugation. In this context, however, the individual contributions are meaningless because their magnitude is smaller than the anticipated error limits.

Selection of conformation pairs for the two-point method was guided by two principles, that (1) conformation A have two methyl hydrogen bonds and be near the lowest-energy configuration, and (2) rotation of a methyl group gives a conformation B that broaches the steep methyl bond breaking "wall" in Figure 4 and resembles Figure 2b. Table 4 presents the results using three pairs of conformations. We see that these results agree well with each other. The traditional hydroxyl-donated bond is assigned strength of about 26 kJ/mol, and when both weak methyl hydrogen bonds exist, they store about 5 kJ/mol each. The total cooperative effect is about 2 kJ/mol, that is, when one methyl hydrogen bond is broken, conformational changes result in loss of only about 3 kJ/mol of stability.

This method requires only a few calculations to estimate hydrogen bond energies and cooperative effects. However, one cannot know for certain if a particular rotation completely removes all the interactions being measured. For example, the hyperconjugation that causes gauche effects[21] are not accounted for by this kind of calculation.

3.4. Energies of the Hydrogen Bond Network: Perturbed Structural Response Method. A more balanced approach to assigning the total binding energy among hydrogen bonds in the network we call the perturbed structural response (PSR) method. Here we take into account all the data points on the methyl rotation grid. A systematic perturbation has been imposed on the system, and the structure has been allowed to respond. The interaction energy is now plotted as a function of dependent variables which describe the response and are amenable to a meaningful physical interpretation.

Figure 6a depicts the distribution of R_1 and R_2 that resulted from perturbing the lowest-energy configuration by imposing methyl rotations in the relaxed PES. Note that all the conformations can be neatly grouped into one of two approximately linear branches along the left and bottom edges of the graph, or within a roughly square region with corners at (R_1, R_2) = (2.3 Å, 2.3 Å) and (3.1 Å, 3.1 Å). Figure 6b gives a detailed view of the crowded square region. The nature of the (R_1, R_2) domain, that it is one-dimensional in some regions and two-dimensional in others makes a true three-dimensional perspective rendering of Figure 6a difficult to read. Therefore, ΔE of each conformation, rounded to the nearest kJ/mol, is portrayed using symbols, so that each different symbol approximately indicates the path of an energy contour. Because the error limits to ΔE are not less than 1−2 kJ/mol (as discussed later), more precise positioning of the energy contours is unnecessary.

The left branch in Figure 6a corresponds to conformations with only methyl-1 forming a weak hydrogen bond, and the bottom branch corresponds to only methyl-2 forming a weak hydrogen bond. The square indicates the region of conformations with two methyl hydrogen bonds, showing the transition from conformers with two stable methyl hydrogen bonds at the lower left corner, to the upper right corner in which both methyl hydrogen bonds are stretched to the breaking point. Further perturbation of either bond causes one of the methyl groups to swing away from EG, allowing the distance between the other methyl hydrogen and O_1 to shorten into a well-formed methyl hydrogen bond in the bottom or left branches of Figure 6. The figure provides clear phenomenological grounds for defining the range of distances for weak methyl hydrogen bonds in this complex to be between 2.3 and 3.1 Å, corresponding to the coordinates of the square.

Figure 6 illustrates a methodology that may prove useful for other weakly interacting systems. Its utility is that each of the three variables, R_1, R_2 and ΔE, is a dependent variable, and together they describe the response of the system to the perturbation. The figure not only depicts the relation of ΔE to R_1 and R_2, but also the range of R_1 and R_2 behaviors the system produces. In this case, the range of (R_1, R_2) behavior clarifies the system response more clearly than does the energy or its relation to R_1 and R_2.

Having defined methyl hydrogen bonds in terms of internuclear distance from the distribution of behaviors, we can understand the energetics of methyl hydrogen bonding by looking at the dependence of ΔE on R_1 and R_2. The difference in energy between the conformers at the lower left corner, with the shortest and strongest methyl hydrogen bonds, and at the upper right corner, with the weakest and longest methyl

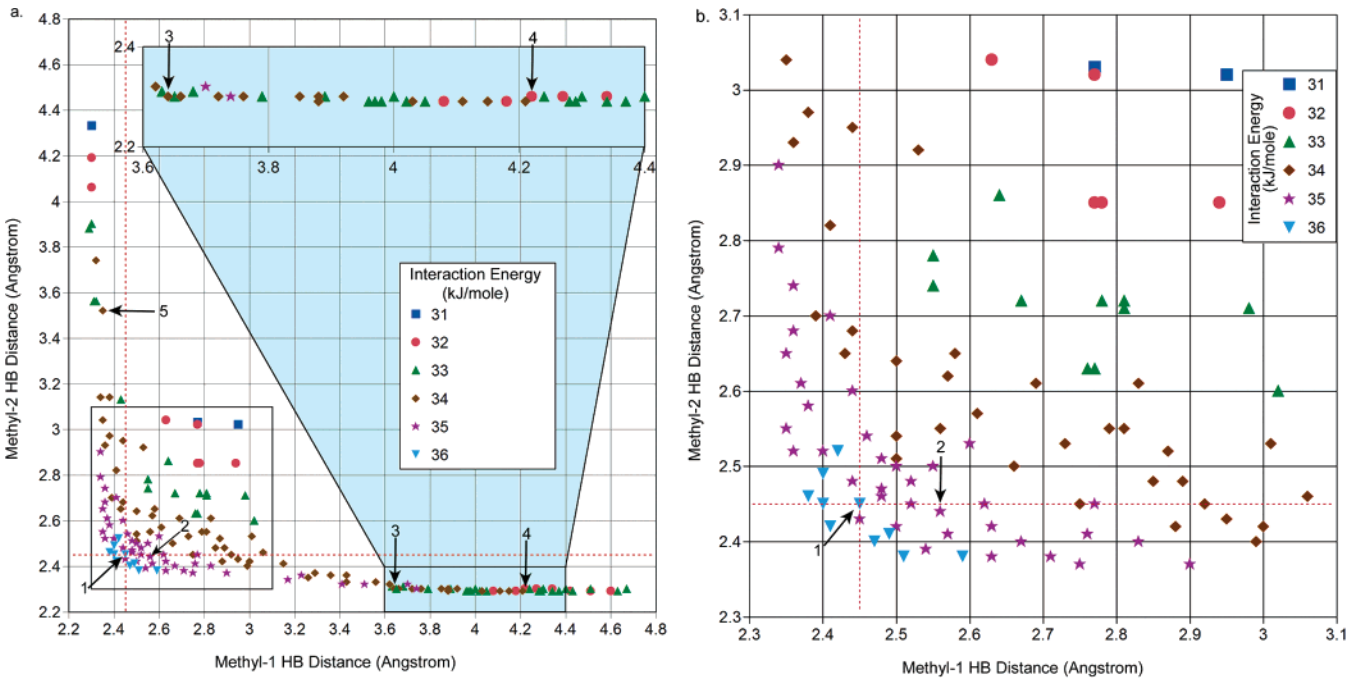

Figure 6. (a) Perturbed structural response diagram depicting interaction energies and distribution of methyl hydrogen−hydroxyl oxygen distances in response to methyl rotation perturbation of 1,2-ethanediol−dimethyl sulfoxide. Includes inset expansion plot of lower linear region. (b) Detailed view of region with R_1 and R_2 between 2.3 and 3.1 Å. Labeled conformations are: 1 = (68°, 174°), lowest-energy; 2 = (68°, 134°), transitional; 3 = (68°, 124°), cooperative methyl-2 H bonded; 4 = (68°, 104°), extreme methyl-2 H bonded; 5 = (78°, 224°), methyl-1 H bonded.

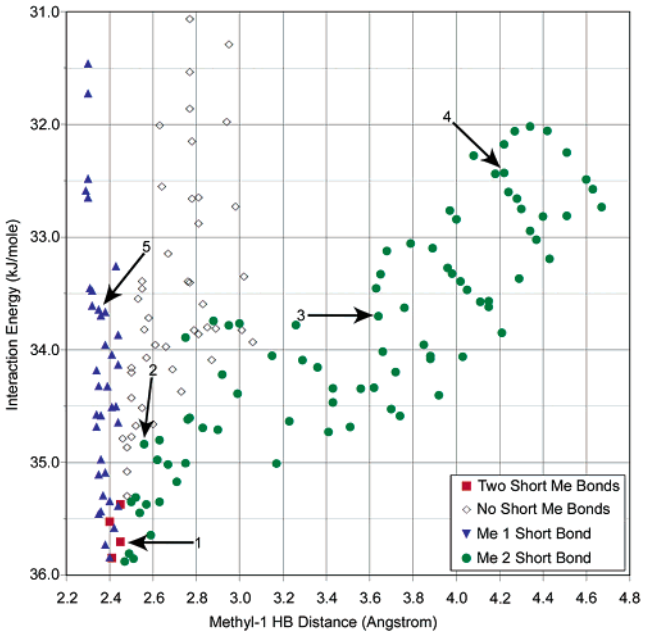

Figure 7. Interaction energy as a function of methyl-1 hydrogen bonding distance, R_1, in 1,2-ethanediol−dimethyl sulfoxide. Labeled conformations are: 1 = (68°, 174°), lowest-energy; 2 = (68°, 134°), transitional; 3 = (68°, 124°), cooperative methyl-2 H bonded; 4 = (68°, 104°), extreme methyl-2 H bonded; 5 = (78°, 224°), methyl-1 H bonded.

hydrogen bonds, is about 5 kJ/mol. Further perturbation breaks a methyl hydrogen bond. Thus we infer that the energy of a weak methyl hydrogen bond is about 5 kJ/mol.

Another way to get at the hydrogen bond energies is to examine the difference in ΔE between the most stable configuration with two weak methyl hydrogen bonds and all other conformations having only one such interaction. Figure 7 provides a side view of Figure 6a, projecting onto the R_1-energy coordinate plane. The conformations identified and discussed in connection with Table 3 are explicitly labeled in Figures 6 and 7. Conformations in Figure 7 are denoted with symbols according to whether R_1 and R_2 are shorter than in the lowest-energy configuration, 2.45 Å. The dashed red horizontal and vertical lines in Figure 6, a and b, divide the data points in this way for Figure 7. In Figure 7, comparing ΔE values with only short methyl-2 distances (denoted with circles) to ΔE with both methyl hydrogen bonds short (denoted with squares) then gives the energy of the methyl-1-donated hydrogen bond. Done as a function of R_1 it displays the energy profile for the breaking of this bond.

The total energy lost in breaking the methyl-1-donated hydrogen bond is about 4 kJ/mol (contrasted to 5 kJ/mol by the two-point method), and is achieved when R_1 reaches about 4.4 Å. But the methyl-1 group has already swung away from contact with atom O_{v1}, by the time R_1 reaches 3.1 Å. As far out as 3.6 Å, ΔE for the complex reaches a plateau with about half of the bond energy remaining, due to the cooperative effects. That this corresponds to the 2 kJ/mol cooperative energy calculated in Table 4 is made clear by finding the first four representative structures given in Table 3, indicated in Figure 7 with integer labeled arrows. Figure 8 shows much the same story for the breaking of the methyl-2-donated hydrogen bond, with a total binding energy for the points indicated with triangles of about 5 kJ/mol and a cooperative effect of 2−3 kJ/mol. The conclusions from Figure 8 are somewhat more equivocal than from Figure 7, because the relevant data series is less well populated.

3.5. Error Limits and Sources of Error. It is necessary to discuss the limitations of the present study in terms of the error inherent in the interaction energies and their differences. On the basis of the considerations in subsection 2.1, and our review of published results comparing the B3PW91 to experimental

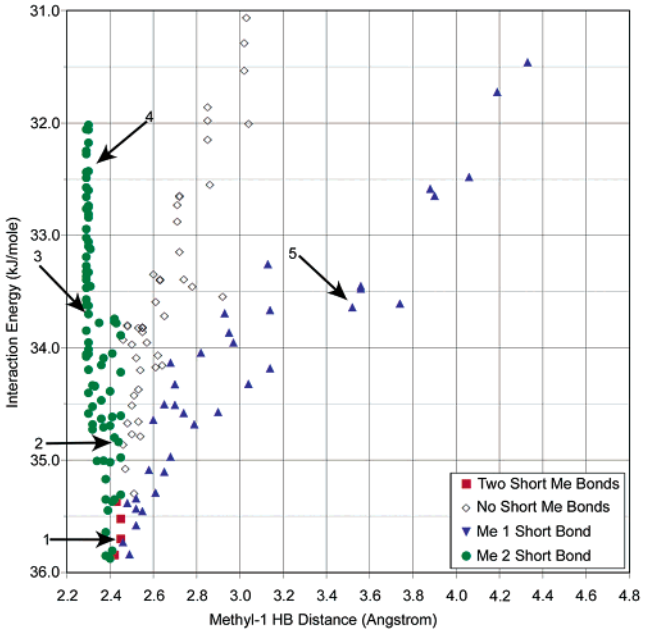

Figure 8. Interaction energy as a function of methyl-2 hydrogen bonding distance, R_2, in 1,2-ethanediol−dimethyl sulfoxide. Numerically labeled conformations are as in Figure 7.

and MP2 results, our best estimate of the error in our model chemistry is about 5 kJ/mol for interaction energies. Thus, we conclude that the total ΔE of the complex is 35 ± 5 kJ/mol.

The uncertainty indicated by the spread of the points in each data series of Figure 6, and the vertical scatter at long distances in Figures 7 and 8 indicate a precision of about $\pm$ 1 kJ/mol in the interaction energies reported there. Applying a 2σ criterion to the data of Table 4 gives a similar estimate. The scatter in Figures 7 and 8 probably results from systematic errors in the convergence to minimum energy conformations in the relaxed potential energy scan. Particularly in regions of configuration space where weak hydrogen bonds break and the methyl groups swing away from EG, the energy is not very sensitive to conformation changes. The complexes are "floppy," as discussed in subsection 2.2. The use of differing convergence criteria in the software, one for "floppy" conditions, and one otherwise, leads to inconsistency in the values of R_1 and R_2 in these regions, and consequent scatter in the energy. In some cases convergence to a local rather than the absolute minimum undoubtedly also contributes.

The history of quantum chemistry teaches us that useful results and chemical insights were achieved via quantum methodology long before those methods were able to achieve "chemical accuracy" of 4−8 kJ/mol. This was largely the result of model error cancellation: when subtracting to get ΔE, systematic errors in the model chemistry often largely canceled each other. Due care is necessary in clearly stating the assumptions on which conclusions are based, but one should not refrain from drawing reasonable and insightful conclusions from calculations.

An analogous situation seems to occur in these calculations. That the precision of the interactions is smaller than the estimated accuracy suggests that significant cancellation of model error occurs when the interaction energies are subtracted. We therefore estimate the error limits for the individual hydrogen bond energies ($E_{mod} = 26$, $E_{weak} = 5$, and $E_{coop} =$ 2−3 kJ/mol) to be double the scatter in the ΔE values, or about $\pm$ 2 kJ/mol. Thus there is evidence of the existence of a cooperative effect among networks of such hydrogen bonds, though the magnitude of the effect calculated here should be considered only an order of magnitude.

3.6. Implications of the Results. Our conclusions are important in several areas of chemistry. First of all, we confirm the results[2] of Vargas, et. al., that methyl groups are capable donators of hydrogen bonds. This contradicts most beginning chemistry textbooks, which focus heavily on electronegative elements as donators. More emphasis should be given to the polarity of the covalent bond donating hydrogen in the context of surrounding functional groups.

Our results also clarify the energy reported in ref 2 of 8.8 kJ/mol for $C^{\alpha}H\cdot\cdot O{=}C$ hydrogen bonds in the context of proteins. In light of our work, it is plausible that $C^{\alpha}H\cdot\cdot O{=}C$ hydrogen bonds form cooperative networks with stronger hydrogen bonds or with each other, and breaking one such interaction may not release the full bond energy. Such bond energies are probably not additive, and so have limited meaning. The importance of such methyl interactions may be precisely in their ability to act cooperatively with stronger hydrogen bonds. To use an analogy from electronics, they could function as binary switches or relays between low energy configurations. This possibility needs to be examined explicitly in subsequent research on $C^{\alpha}H\cdot\cdot O{=}C$ hydrogen bonds. Our work suggests specific structural changes to look for as elements of that cooperativity.

This work provides the basis for a model to understand another ubiquitous phenomenon of biochemistry. It is well-known that in protein folding there are frequently semi-stable conformations that slow or prevent the folding of a protein into its native configuration.[22] Because the cooperative effect calculated here is very close to RT, the thermal energy available to a degree of conformational freedom, cooperative effects of C^{α} or methyl hydrogen bonds may have a significant role in this phenomenon. One can envision a scenario in which a functional group swinging away on breaking a C^{α} or methyl hydrogen bond would act as a switch or chemico-mechanical relay which permits or blocks a residue from reaching its native configuration. More generally, the existence of cooperative effects on the order of RT in networks of hydrogen bonds should be considered in studying protein folding and the behavior of reactive sites. In fact, networks of hydrogen bonds may be biologically important precisely because they are capable of a variety of cooperative arrangements for storing energy among the bonds, while the complex undergoes a precisely limited range of structural movement.

Finally, cooperative effects in a network of hydrogen bonds have been clearly demonstrated. This should clarify our thinking about hydrogen bonding. In many cases, it may not be sufficient only to measure or calculate the strength of a hydrogen bond. One should consider the many subtle structural degrees of freedom available at relevant temperatures that can result in cooperative effects, and develop means of detecting cooperativity. The PSR method represents a new way of doing this.

(22) See, for example: Sall, A.; Shakhnovich, E.; Karplus, M. *Nature* **1994**, *369*, 248.

Conclusions

The 1:1 gas-phase complex of 1,2-ethanediol and dimethyl sulfoxide is stabilized by a network of three hydrogen bonds, including two bonds donated by methyl groups. Evidence of methyl donation in this case includes: (1) hydrogen−acceptor internuclear distances, (2) hydrogen bond angles, (3) clues in the geometric configuration suggesting an energetic advantage to the association of both methyl groups with the hydroxyl oxygen, and (4) electrostatic evidence.

The complex has an attractive interaction of 36 ± 5 kJ/mol in the B3PW91/6-311++G**//B3PW91/6-31+G** model chemistry. Hydrogen-bond energies in a network are not additive. The three hydrogen bonds cooperate in such a way that when a methyl-donated bond is broken, under some conditions specific structural adaptations absorb 2−3 kJ/mol of energy formerly stored by the broken hydrogen bond. When both methyl bonds are intact, the O−H··O−S interaction has strength of 26 ± 2 kJ/mol, and each methyl-donated bond stores 5 ± 2 kJ/mol.

Acknowledgment. R.V. thanks the reviewers for helpful suggestions, and the University of North Florida Training and Service Institute for partial summer financial support.

Supporting Information Available: Cartesian coordinates of all reported conformations, internal coordinates of conformations described in Table 3, and numerical values represented in Figures 3−8, as well as energies and other hydrogen bond properties for all conformations. This material is available free of charge via the Internet at http://pubs.acs.org.

JA036516A